Available online at www.sciencedirect.com
SCIENCE DIRECT
Journal of Organometallic Chemistry 691 (2006) 2666–2678
Journal of Organometallic Chemistry
www.elsevier.com/locate/jorganchem

From halo-azasilylenes to halo-phosphasilylenes (X-CNSi vs. X-CPSi) at ab initio and DFT levels

M.Z. Kassaee *, S.M. Musavi, M. Ghambarian

Department of Chemistry, Tarbiat Modarres University, P.O. Box 14155-4838, Tehran, Iran

Received 24 November 2005; received in revised form 31 January 2006; accepted 31 January 2006
Available online 20 March 2006

Abstract

The higher the electropositivity of the substituents has been associated with the higher possibility of encountering a triplet ground state silylene [P.P. Gaspar, M. Xiao, D. Ho Pae, D.J. Berger, T. Haile, T. Chen, D. Lei, W.R. Winchester, P. Jiang, J. Organomet. Chem. 646 (2002) 68]. Here, going from the reported halo-azasilylenes X-CNSi [M.Z. Kassaee, S.M. Musavi, H. Hamadi, M. Ghambarian, S.E. Hosseini, J. Mol. Struct. (Theochem) 730 (2005) 33] to the analogues more electropositively substituted halo-phosphasilylenes X-CPSi has reduced the chances of encountering triplet ground state silylenes (X = H, F, Cl and Br). Even though all singlet isomers seem to be more stable than their corresponding triplets, singlet–triplet cross over diagrams may help the future design of new acyclic triplet state silylenes.

Keywords: Triplet silylene; HOMO–LUMO; HCPSi; FCPSi; ClCPSi; BrCPSi; Phosphasilacyclopropenylidene; [(Phosphino)methylene]silylene; Methylidynphosphinesilylene; Ab initio; DFT

1. Introduction

Considerable studies are focused on the structures and reactions of silylenes and related group-14 divalent species [1–13]. Generally, all known silylene species possess a singlet (**s**) ground state, in contrast to their carbene analogues which often have triplet (**t**) ground states. This has made the quest for triplet ground state silylenes one of the most challenging issues in the modern organosilicon chemistry [14]. Theoretical studies indicate that substituents attached to the divalent center have considerable effects on the singlet–triplet energy gaps ($\Delta E_{\mathbf{s\text{-}t}}$) [14–16]. It has been shown that electronegative substituents increase the $\Delta E_{\mathbf{s\text{-}t}}$, whereas electropositive substituents decrease the gap. In addition, π-donor or π-acceptor substituents exert a significant effect on $\Delta E_{\mathbf{s\text{-}t}}$. This is in a way that π-donor substituents stabilize singlet states while π-acceptor substituents stabilize triplet states. For instance, the $^3B_1$ state of SiH_2 is 18–23 kcal/mol [17,18] higher in energy than the $^1A_1$ ground state, whereas a much larger gap of 75–77 kcal/mol has been measured for SiF_2 [19]. Likewise, methyl substituents increase the gap to 23–26 kcal/mol in $Si(CH_3)_2$ [20,21]. In contrast, the more electropositive SiH_3 group decreases the calculated $\Delta E_{\mathbf{s\text{-}t}}$ to −5 to −10 kcal/mol in $Si(SiH_3)_2$ [16,22]. With electropositive Li substitution, was predicted that SiLiH and $SiLi_2$ are ground-state triplets, being by several kcal/mol more stable than their corresponding singlet species [15,20,23,24]. Holthausen et al. have provided a theoretical prescription of how to generate the first triplet ground state silylene [22,25]. Afterward, a Japanese group realized this prediction by synthesis and EPR confirmation of bis(tri-*tert*-butylsilyl)silylene [26]. Moreover, four triplet silylenes were found beyond the potential energy surface (PES) of monohalogenated H_2Si_3 silylenes [27], while on the PES of its analogous C_2H_2Si no triplet silylenes were observed [28]. We have already reported the calculated thermodynamic data on 24 isomers of haloazasilylenes

* Corresponding author. Tel.: +011 98 912 100392; fax: +98 21 88006544.
E-mail addresses: Kassaeem@Modares.ac.ir, drkassaee@yahoo.com (M.Z. Kassaee).

0022-328X/$ - see front matter © 2006 Elsevier B.V. All rights reserved.
doi:10.1016/j.jorganchem.2006.01.059

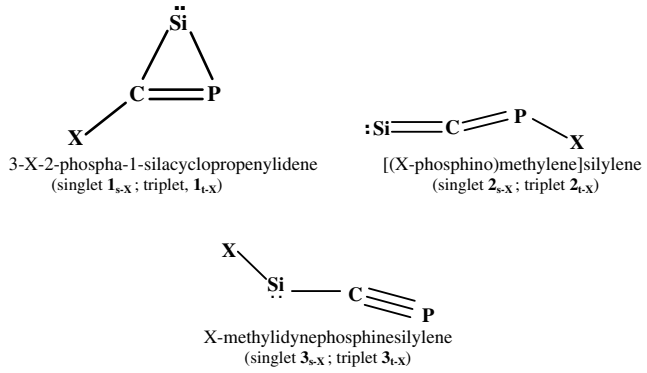

Fig. 1. The three most significant structures considered for singlet (**s**) and triplet (**t**) phosphasilylenes, X-CPSi (**1**, **2** and **3**, where X = H, F, Cl and Br).

X-CNSi, where only triplet H–N=C=Si silylene appeared to be more stable than its corresponding singlet state [29]. In attempt to boost the chances of encountering triplet ground state silylenes we have switched to the analogous halophosphasilylenes X-CPSi where the higher electropositivity of phosphorous (than nitrogen) was predicted to be a help. Moreover, great attentions have been paid to the chemistry of silicon and phosphorus, due to their attendance in the astrophysical chemistry as well as their microelectronic and photo-electronic applications [30,31]. Hence, in this manuscript silylenic structures of H–CPSi, F–CPSi, Cl–CPSi and Br–CPSi formula in their singlet and triplet states are examined, using detailed ab initio and DFT calculations (see Fig. 1). These molecules are concurrently involving interesting bonding properties [32–39].

2. Computational methods

All calculations, in this paper are performed using the GAUSSIAN 98 program package [40]. The geometries and energetics of singlet and triplet H–CPSi silylenes, as well as their halogen substituted analogues: F–CPSi, Cl–CPSi and Br–CPSi, are calculated using standard quantum chemical ab initio and DFT methods. These X-CPSi species are confined to three skeletal arrangements including: 3-X-2-phospha-1-silacyclopropenylidene (**1**), [(X-phosphino)methylene]silylene (**2**), and X-methylidynephosphinesilylene (**3**). Full optimizations are preformed without any symmetrical restrictions. In some cases final optimized structures are drastically different with the input structures. For DFT calculations the Becke's hybrid one-parameter and three-parameter functional are employed, using the LYP correlation [41,42] with the 6-311++G** basis set. For the second-order MØller–Plesset (MP2) method 6-311++G** basis set and for the third-order MØller–Plesset (MP3) method the 6-311+G* basis set is employed [43,44]. In order to improve the energetic predictions, the MP2/6-311++G** optimized geometries are submitted as input for single-point calculations at MP4, QCISD(T) and CCSD(T) levels with 6-311++G** basis sets [45–48]. Singlet states are calculated with spin-restricted wave functions. Triplet states are calculated using the unrestricted formalisms. The harmonic vibrational frequencies and zero point energies (ZPE) are calculated on the MP2 and B3LYP optimized structures, at the same level used for their optimization. The vibrational frequencies and ZPE data at the HF, B3LYP and MP2 are scaled by 0.89, 0.98 and 0.92, respectively [49,50]. This is to account for the differences between the harmonic and anharmonic oscillations of the actual bonds. The NBO population analysis are accomplished at the B3LYP/6-311++G** level, for all silylenic structures [51].

3. Results and discussion

We begin with listing our results, before discussing them. The singlet (**s**) and triplet (**t**) of silylenes X-CPSi consisting of H–CPSi, F–CPSi, Cl–CPSi and Br–CPSi, are described in three structures including: 3-X-2-phospha-1-silacyclopropenylidene (**1**), [(X-phosphino)methylene]silylene (**2**), and X-methylidynphosphinesilylene (**3**) (see Fig. 1). Thermodynamic data are calculated at eight ab initio and DFT levels of theory including: HF/6-311+G**, B1LYP/6-311++G**, B3LYP/6-311++G**, MP3/6-311+G*, MP2/6-311++G**, MP4(SDTQ)/6-311++G**, QCISD(T)/6-311++G** and CCSD(T)/6-311++G** (X = H, F, Cl and Br) (see Tables 1–4). These calculation methods show a rather conspicuous consistency in calculating the relative energies of the 24 structures (see Tables 1–4). Optimized geometrical parameters of **1** through **3** are reported, using MP2/6-311++G** and B3LYP/6-311++G** levels of theory; where bond lengths are given in angstrom and bond angles in degrees (shown in *italics*, Fig. 2). Similar results are obtained for the geometrical parameters optimized through methods other than B3LYP/6-311++G** and MP2/6-311++G** which are not included in Fig. 2. All optimized structures appear planar with C_s symmetry. Two structures including: $\mathbf{1}_{\mathbf{t\text{-}F}}$ (optimized at B3LYP/6-311++G**) and $\mathbf{1}_{\mathbf{t\text{-}H}}$ (optimized at MP2/6-311++G**) ruptured through optimization (see Fig. 3). For both singlet and triplet isomers of X-CPSi, the energies of the highest occupied molecular orbitals (HOMO) and the lowest unoccupied molecular orbitals (LUMO) are obtained through NBO analysis [51] (see Fig. 4). The B3LYP/6-311++G** calculated LUMO–HOMO energy gaps of the singlet X-CPSi silylenes, appear to have a linear relationship with their corresponding singlet–triplet energy separations, $\Delta E_{\mathbf{s\text{-}t,X}}$, where halogens appear to increase the magnitude of LUMO–HOMO energy gaps. The linearity trend is: $\mathbf{2}_{\mathbf{s\text{-}X}}$ ($R^2 = 0.98$) > $\mathbf{3}_{\mathbf{s\text{-}X}}$ ($R^2 = 0.97$) > $\mathbf{1}_{\mathbf{s\text{-}X}}$ ($R^2 = 0.65$), where R^2 = correlation coefficient. The order of LUMO–HOMO energy gaps as a function of substituents X for silylenes **1**–**3** follows the electro-negativity: F > Cl > Br > H.

The eight different ab initio and DFT calculation methods employed in this work show similar orders of relative

Table 1
Relative energies (kcal/mol), with ZPE corrections, for singlet $\mathbf{1}_{s\text{-}H}$, $\mathbf{2}_{s\text{-}H}$ and $\mathbf{3}_{s\text{-}H}$ as well as triplet states $\mathbf{1}_{t\text{-}H}$, $\mathbf{2}_{t\text{-}H}$ and $\mathbf{3}_{t\text{-}H}$ of silylenic H-CPSi; calculated at eight levels of theory; along with dipole moments (Debye) and vibrational zero point energies (kcal/mol), calculated at B3LYP/6-311++G**

Structure	Relative energies (kcal/mol)								Dipole moments (*D*)	Vibrational zero point energies (kcal/mol)
	HF/ 6-311++G**	MP36-311++G**[a]	B1LYP/ 6-311++G**	B3LYP/ 6-311++G**	MP2/ 6-311++G**[a]	MP4(SDTQ)/ 6-311++G**[a]	QCISD(T)/ 6-311++G**[a]	CCSD(T)/ 6-311++G**[a]	B3LYP/ 6-311++G**	B3LYP/ 6-311++G**
$\mathbf{1}_{s\text{-}H}$	0.00	0.00	0.00	0.00	0.00	0.00	0.00	0.00	0.57	10.08
$\mathbf{1}_{t\text{-}H}$	12.15	41.71	33.07	33.85	22.09	44.98	38.48	38.66	1.29	8.81
$\mathbf{2}_{s\text{-}H}$	31.62	36.51	28.86	28.92	35.21	31.60	31.00	31.10	0.36	7.76
$\mathbf{2}_{t\text{-}H}$	32.28	60.19	44.10	44.65	64.79	59.08	52.68	53.15	0.59	7.23
$\mathbf{3}_{s\text{-}H}$	17.51	25.41	18.76	19.07	21.48	19.03	19.59	19.75	0.27	7.31
$\mathbf{3}_{t\text{-}H}$	15.32	53.56	38.11	38.61	55.70	52.98	43.08	43.65	0.95	7.34

[a] ZPE not included.

Table 2
Relative energies (kcal/mol), with ZPE corrections, for singlet $\mathbf{1}_{s\text{-}F}$, $\mathbf{2}_{s\text{-}F}$ and $\mathbf{3}_{s\text{-}F}$ as well as triplet states $\mathbf{1}_{t\text{-}F}$, $\mathbf{2}_{t\text{-}F}$ and $\mathbf{3}_{t\text{-}F}$ of silylenic F-CPSi; calculated at eight levels of theory; along with dipole moments (Debye) and vibrational zero point energies (kcal/mol), calculated at B3LYP/6-311++G**

Structure	Relative energies (kcal/mol)								Dipole moments (*D*)	Vibrational zero point energies (kcal/mol)
	HF/ 66-311+G*	MP3/ 311++G**[a]	B1LYP/ 6-311++G**	B3LYP/ 6-311++G**	MP2/ 6-311++G**[a]	MP4(SDTQ)/ 6-311++G**[a]	QCISD(T)/ 6-311++G**[a]	CCSD(T)/ 6-311++G**[a]	B3LYP/ 6-311++G**	B3LYP/ 6-311++G**
$\mathbf{1}_{s\text{-}F}$	35.85	31.27	31.12	30.28	34.98	34.94	34.12	34.00	1.18	5.62
$\mathbf{1}_{t\text{-}F}$	56.47	84.24	73.73	73.79	95.76	91.41	82.23	82.25	1.12	4.38
$\mathbf{2}_{s\text{-}F}$	36.18	34.86	30.32	29.76	37.76	36.55	35.71	35.75	2.45	4.79
$\mathbf{2}_{t\text{-}F}$	50.06	75.10	63.62	64.06	86.79	82.08	73.68	73.90	2.26	4.17
$\mathbf{3}_{s\text{-}F}$	0.00	0.00	0.00	0.00	0.00	0.00	0.00	0.00	1.92	4.78
$\mathbf{3}_{t\text{-}F}$	17.21	48.32	36.70	36.70	53.56	54.16	44.22	44.55	1.44	4.84

[a] ZPE not included.

Table 3
Relative energies (kcal/mol), with ZPE corrections, for singlet $\mathbf{1}_{s\text{-}Cl}$, $\mathbf{2}_{s\text{-}Cl}$ and $\mathbf{3}_{s\text{-}Cl}$ as well as triplet states $\mathbf{1}_{t\text{-}Cl}$, $\mathbf{2}_{t\text{-}Cl}$ and $\mathbf{3}_{t\text{-}Cl}$ of silylenic Cl-CPSi; calculated at eight levels of theory; along with dipole moments (Debye) and vibrational zero point energies (kcal/mol), calculated at B3LYP/6-311++G**

Structure	Relative energies (kcal/mol)								Dipole moments (*D*)	Vibrational zero point energies (kcal/mol)
	HF/ 6-311++G**	MP3/ 6-311+G*[a]	B1LYP/ 6-311++G**	B3LYP/ 6-311++G**	MP2/ 6-311++G**[a]	MP4(SDTQ)/ 6-311++G**[a]	QCISD(T)/ 6-311++G**[a]	CCSD(T)/ 6-311++G**[a]	B3LYP/ 6-311++G**	B3LYP/ 6-311++G**
$\mathbf{1}_{s\text{-}Cl}$	23.42	16.87	19.16	18.51	17.46	18.55	18.48	18.33	0.98	4.82
$\mathbf{1}_{t\text{-}Cl}$	39.82	64.37	55.54	58.16	83.82	69.82	62.00	62.05	1.35	3.71
$\mathbf{2}_{s\text{-}Cl}$	32.16	30.12	25.49	24.96	32.93	31.82	30.75	30.78	2.83	4.22
$\mathbf{2}_{t\text{-}Cl}$	41.67	64.56	53.69	54.10	75.68	71.23	63.81	64.01	2.26	3.69
$\mathbf{3}_{s\text{-}Cl}$	0.00	0.00	0.00	0.00	0.00	0.00	0.00	0.00	2.03	4.27
$\mathbf{3}_{t\text{-}Cl}$	11.76	42.73	32.00	32.10	48.58	48.43	38.27	38.60	1.07	4.33

[a] ZPE not included.

Table 4
Relative energies (kcal/mol), with ZPE corrections, for singlet $\mathbf{1}_{s\text{-}Br}$, $\mathbf{2}_{s\text{-}Br}$ and $\mathbf{3}_{s\text{-}Br}$ as well as triplet states $\mathbf{1}_{t\text{-}Br}$, $\mathbf{2}_{t\text{-}Br}$ and $\mathbf{3}_{t\text{-}Br}$ of silylenic Br-CPSi; calculated at eight levels of theory; along with dipole moments (Debye) and vibrational zero point energies (kcal/mol), calculated at B3LYP/6-311++G**

Structure	Relative energies (kcal/mol)								Dipole moments (*D*)	Vibrational zero point energies (kcal/mol)
	HF/ 6-311++G**	MP3/ 6-311+G*[a]	B1LYP/ 6-311++G**	B3LYP/ 6-311++G**	MP2/ 6-311++G**[a]	MP4(SDTQ)/ 6-311++G**[a]	QCISD(T)/ 6-311++G**[a]	CCSD(T)/ 6-311++G**[a]	B3LYP/ 6-311++G**	B3LYP/ 6-311++G**
$\mathbf{1}_{s\text{-}Br}$	22.94	17.50	18.69	18.09	17.29	18.38	18.54	18.38	0.98	4.51
$\mathbf{1}_{t\text{-}Br}$	36.93	59.85	49.21	49.11	31.91	64.20	57.07	57.15	0.70	3.47
$\mathbf{2}_{s\text{-}Br}$	30.17	27.77	23.26	22.74	30.43	29.35	28.28	28.32	2.82	4.06
$\mathbf{2}_{t\text{-}Br}$	38.67	60.51	49.95	50.32	71.32	89.10	51.27	55.15	1.95	3.53
$\mathbf{3}_{s\text{-}Br}$	0.00	0.00	0.00	0.00	0.00	0.00	0.00	0.00	1.97	4.09
$\mathbf{3}_{t\text{-}Br}$	10.62	41.56	30.80	30.93	47.76	47.33	37.04	37.37	0.83	4.11

[a] ZPE not included.

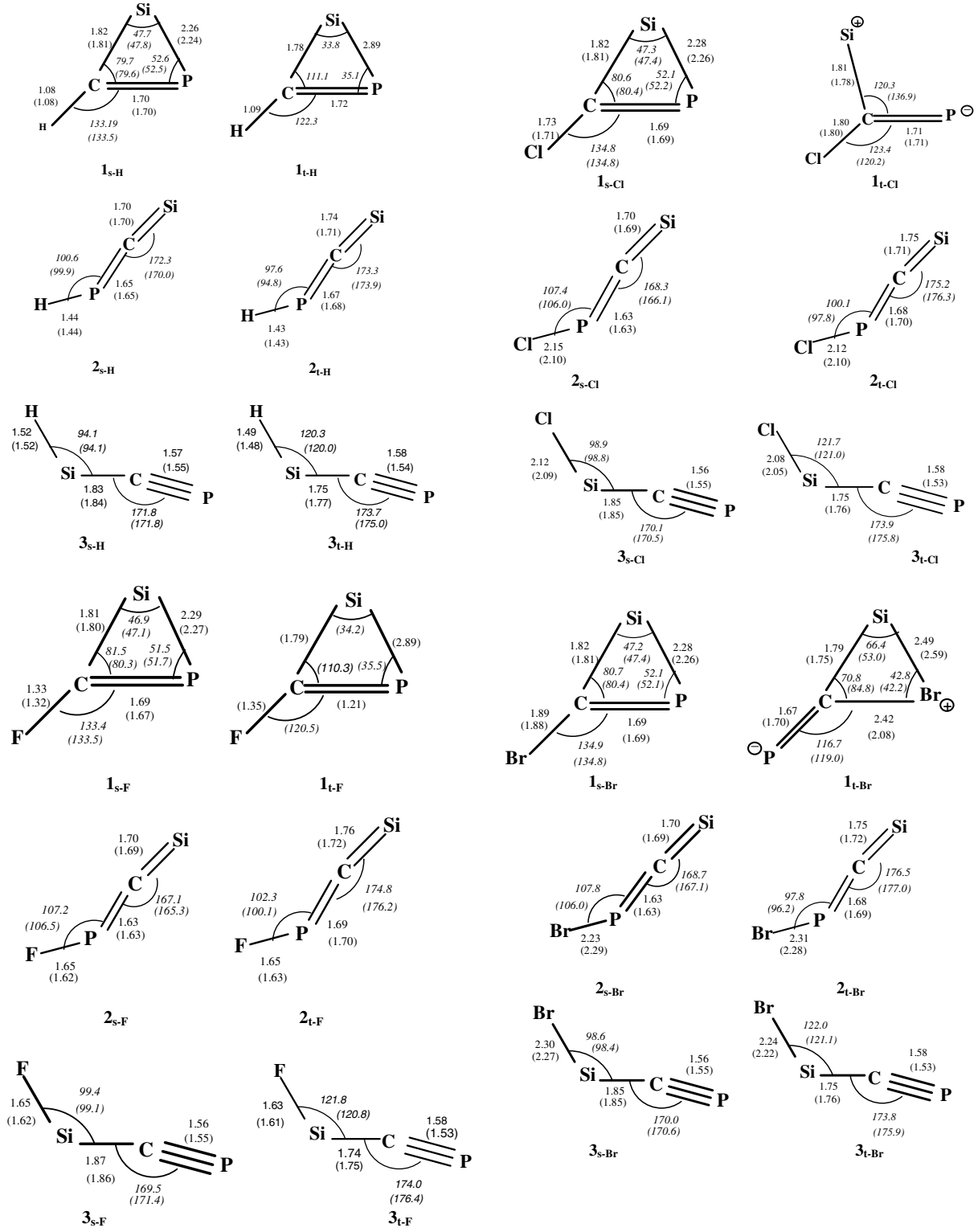

Fig. 2. Selected geometrical parameters for 24 silylenic X-CPSi, where bond lengths are given in Å and *bond angles* in degrees (X = H, F, Cl, Br). Data are computed at two levels of theory: B3LYP/6-311++G** and MP2/6-311++G** (in parentheses).

energies. Nevertheless, the calculated relative energies themselves appear sensitive to the level of theory employed (see Tables 1–4). As anticipated, the HF calculated energies appear vastly far from those of the more time consuming (rather more advanced) methods employed. Also, the relative energies, calculated at QCISD(T) and CCSD(T) levels, are quite similar to each other, close to DFT results, while they appear 2–10 kcal/mol different from those of MP4. Hence, in this work CCSD(T)/6-311++G** is chosen over other calculation methods in the energy discussion.

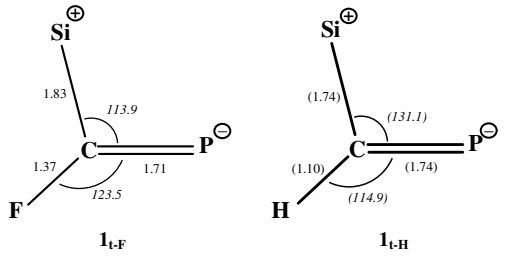

$\mathbf{1_{t\text{-}F}}$ $\mathbf{1_{t\text{-}H}}$

Fig. 3. Ruptured optimized structures for $\mathbf{1_{t\text{-}F}}$ (at B3LYP/6-311++G**) and for $\mathbf{1_{t\text{-}H}}$ (at MP2/6-311++G**). Bond lengths are given in Å and *bond angles* in degrees (°).

Results of NBO calculations involved atomic charges along with the bond orders at B3LYP/6-311++G** level for three structures of X-CPSi silylenes are presented (see Table 5). Harmonic vibrational frequencies are computed on each MP2 and B3LYP optimized structures. This not only serves to estimate the zero-point vibrational energy correction, but also allows assessing the nature of stationary points, confirming that they correspond to the true minima on their potential energy surface. Force constant calculations show no negative force constants for X-CPSi silylenes. So, all silylenic species studied are real isomers. Calculated harmonic frequencies are not provided for the sake of brevity, but are available upon request.

3.1. Structures (*1*–*3*) vs. singlet–triplet energy gaps

3.1.1. Silylenes with cyclic structures (*1*)

Cyclic singlet 3-X-2-phospha-1-silacyclopropenylidene, $\mathbf{1_{s\text{-}X}}$, appear more stable than their corresponding cyclic triplet states, $\mathbf{1_{t\text{-}X}}$, mostly due to the higher aromatic character of the former and a higher P–Si bond strain of the latter (X = H, F, Cl and Br) (see Tables 1–4). These results appear consistent with those of singlet and triplet states of carbenic C_3HX as well as silylenic C_2HXSi and CXNSi analogues [28,29,52]. The CCSD(T)/6-311++G** calculated order of singlet–triplet energy gaps ($\Delta E_{\mathbf{s\text{-}t,X}}$), between $\mathbf{1_{s\text{-}X}}$ and $\mathbf{1_{t\text{-}X}}$ follows electro-negativity of the substituents (X): $\Delta E_{\mathbf{s\text{-}t,F}}$ (48.25 kcal/mol) > $\Delta E_{\mathbf{s\text{-}t,Cl}}$ (43.72 kcal/mol) > $\Delta E_{\mathbf{s\text{-}t,Br}}$ (38.77 kcal/mol) > $\Delta E_{\mathbf{s\text{-}t,H}}$ (38.66 kcal/mol). In this trend, fluorine apparently increases the stability of singlet state more than the others. A rather low energy difference between X = H and F ($\Delta E_{\mathbf{s\text{-}t,F}} - \Delta E_{\mathbf{s\text{-}t,H}} = 9.48$ kcal/mol) is expected, since in cyclic $\mathbf{1_{s\text{-}X}}$ and $\mathbf{1_{t\text{-}X}}$ species, halogens (X) are not directly attached to the silylenic center (see Fig. 1). Discrepancy between $\mathbf{1_{t\text{-}X}}$ geometrical parameters is considerable. For instance, $\mathbf{1_{t\text{-}H}}$ preserves its original cyclic structure through optimization at B3LYP/6-311++G**, while $\mathbf{1_{t\text{-}F}}$ breaks apart at the same level of theory. In contrast, $\mathbf{1_{t\text{-}F}}$ preserves its original cyclic structure through optimization at MP2/6-311++G**, while $\mathbf{1_{t\text{-}H}}$ breaks apart at the same level of theory (see Fig. 2, Table 1). The high relative energy of $\mathbf{1_{t\text{-}H}}$ (38.66 kcal/mol) at B3LYP/6-311++G**, is most likely due to the strain associated with the shrinking of Si–C bond along with the concurrent increase of P–Si bond length to 2.89 Å. In fact, such lengthening is so high that leads to the eventual breakage of P–Si bond, at MP2/6-311++G** level of theory, making cyclic $\mathbf{1_{t\text{-}H}}$ impossible to be optimized without rupture at this level (see Fig. 3). Similarly, the relative energy of $\mathbf{1_{t\text{-}F}}$ is also high (82.25 kcal/mol) with a MP2/6-311++G** calculated P–Si bond length of 2.89 Å. However, according to B3LYP/6-311++G** calculations, P–Si bond also ruptures through optimization, making cyclic

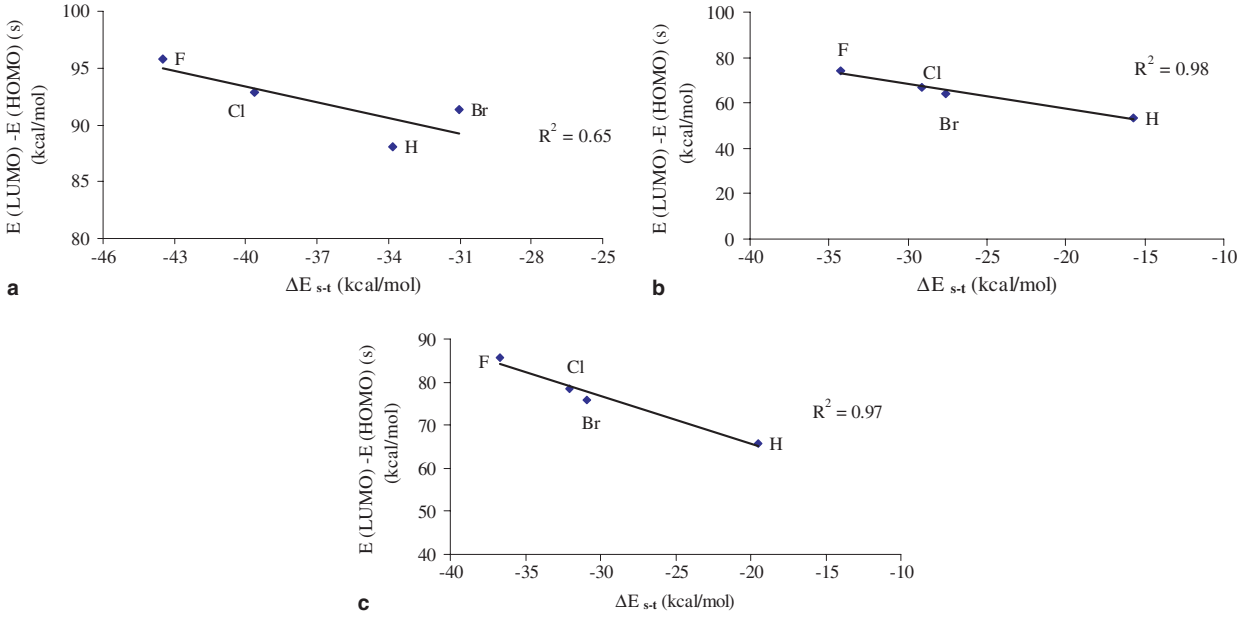

Fig. 4. Correlations (R^2 = correlation coefficient) between the LUMO–HOMO energy gaps (kcal/mol) of the singlet X-CPSi phosphasilylenes (where X = H, F, Cl and Br), against their corresponding singlet–triplet energy separations, $\Delta E_{\mathbf{s\text{-}t}}$ (kcal/mol), calculated at B3LYP/6-311++G** level of theory: $\mathbf{1_{s\text{-}X}}$ vs. $\mathbf{1_{t\text{-}X}}$ (diagram a); $\mathbf{2_{s\text{-}X}}$ vs. $\mathbf{2_{t\text{-}X}}$ (diagram b); and $\mathbf{3_{s\text{-}X}}$ vs. $\mathbf{3_{t\text{-}X}}$ (diagram c).

Table 5
NBO analyses including atomic charges and bond orders of X-CPSi (X = H, F, Cl and Br) phosphasilylenes confined to three structures **1**–**3** calculated at B3LYP/6-311++G**

Structure	Species	Atomic charge				Bond order			
		:Si	C	P	X	C–X	C–P	:Si–C	:Si–P
1	$\mathbf{1}_{s\text{-}H}$	0.59	−1.07	0.27	0.22	1.02	1.83	1.00	0.92
	$\mathbf{1}_{t\text{-}H}$	0.76	−1.42	0.40	0.25	1.01	1.58	1.35	0.39
	$\mathbf{1}_{s\text{-}F}$[a]	0.59	−0.47	0.23	−0.34	–	–	–	–
	$\mathbf{1}_{t\text{-}F}$[a]	0.68	−0.71	0.40	−0.37	–	–	–	–
	$\mathbf{1}_{s\text{-}Cl}$[a]	0.65	−1.03	0.31	0.07	–	–	–	–
	$\mathbf{1}_{t\text{-}Cl}$	0.81	−1.30	0.48	0.01	1.23	1.63	1.27	0.30
	$\mathbf{1}_{s\text{-}Br}$[a]	0.67	−1.14	0.33	0.14	–	–	–	–
	$\mathbf{1}_{t\text{-}Br}$	0.74	−1.22	0.58	−0.10	0.79	1.86	1.17	0.24
						P–X	**C–P**	**:Si–C**	
2	$\mathbf{2}_{s\text{-}H}$	0.87	−1.42	0.62	−0.08	0.87	1.65	1.50	
	$\mathbf{2}_{t\text{-}H}$	0.75	−1.12	0.37	0.00	0.88	1.58	1.52	
	$\mathbf{2}_{s\text{-}F}$	0.98	−1.60	1.20	−0.57	0.79	1.61	1.42	
	$\mathbf{2}_{t\text{-}F}$	0.76	−1.12	0.91	−0.56	0.79	1.43	1.49	
	$\mathbf{2}_{s\text{-}Cl}$	0.98	−1.54	0.89	−0.33	1.02	1.71	1.39	
	$\mathbf{2}_{t\text{-}Cl}$	0.79	−1.12	0.61	−0.28	0.99	1.49	1.47	
	$\mathbf{2}_{s\text{-}Br}$	0.98	−1.53	0.83	−0.27	1.06	1.73	1.37	
	$\mathbf{2}_{t\text{-}Br}$	0.80	−1.14	0.55	−0.20	1.01	1.53	1.47	
						C-P	**Si-C**	**:Si-X**	
3	$\mathbf{3}_{s\text{-}H}$	0.81	−1.19	0.63	−0.25	2.46	0.82	0.68	
	$\mathbf{3}_{t\text{-}H}$	0.80	−1.24	0.59	−0.15	2.34	1.27	0.86	
	$\mathbf{3}_{s\text{-}F}$	1.23	−1.23	0.66	−0.67	2.47	0.72	0.66	
	$\mathbf{3}_{t\text{-}F}$	1.36	−1.36	0.62	−0.63	2.24	1.34	0.69	
	$\mathbf{3}_{s\text{-}Cl}$[a]	0.96	−1.21	0.67	−0.41	–	–	–	
	$\mathbf{3}_{t\text{-}Cl}$[a]	1.00	−1.29	0.62	−0.34	–	–	–	
	$\mathbf{3}_{s\text{-}Br}$[a]	0.89	−1.22	0.68	−0.34	–	–	–	
	$\mathbf{3}_{t\text{-}Br}$[a]	−0.20	−0.59	0.01	−0.22	–	–	–	

[a] Bond orders are not included due to rearrangement of initial structures.

$\mathbf{1}_{t\text{-}F}$ impossible to exist (see Fig. 3). In accordance to all methods of calculations employed, due to P–Si bond breakage, neither $\mathbf{1}_{t\text{-}Cl}$ nor $\mathbf{1}_{t\text{-}Br}$ may exist (see Fig. 2). The reminiscence of the Br possible anchimeric assistance, for the P–Si bond ruptures, is indicated by the formation of a three member cyclic structure, upon optimization of the initial $\mathbf{1}_{t\text{-}Br}$ inputs (see Fig. 2). Such neighboring group participation of bromine may be attributed to its larger size and higher polarizability compared to the chlorine and/or fluorine.

Interestingly, the divalent angles ∠CSiP in the two singlet species $\mathbf{1}_{s\text{-}H}$ and $\mathbf{1}_{s\text{-}F}$ are larger than those in their corresponding triplet states, $\mathbf{1}_{t\text{-}H}$ and $\mathbf{1}_{t\text{-}F}$ (see Fig. 2). This is in contrast to many acyclic carbenes and silylenes, where the singlet divalent angle is found smaller than the corresponding triplet divalent angle [53]. Apparently, halogens exert less perturbation on the aromatic CSiP ring, in the singlet states, than the non-aromatic CSiP ring, in the corresponding triplet states; rendering higher *s* character to the Si atom in the singlet state. In the four singlet $\mathbf{1}_{s\text{-}X}$ species, the B3LYP/6-311++G** calculated trend of the size of ∠CSiP angle is: $\mathbf{1}_{s\text{-}H}$ (47.7°) > $\mathbf{1}_{s\text{-}Cl}$ (47.3°) > $\mathbf{1}_{s\text{-}Br}$ (47.2°) > $\mathbf{1}_{s\text{-}F}$ (46.9°) (see Fig. 2). Hence, the ∠CSiP angle is the largest when X = H. Here, in contrast to hydrogen, which has no non-bonding electrons, halogens have the potential of forming canonical forms for $\mathbf{1}_{s\text{-}X}$ with an exo C=X bond which force an increase in the ∠SiPC angle, on the account of decreasing the size of the ∠CSiP angle (see Scheme 1).

The ∠SiPC is larger in all singlet $\mathbf{1}_{s\text{-}X}$, compared to their corresponding angles in triplet state $\mathbf{1}_{t\text{-}X}$, due to the higher *p* character of P and Si, induced by the singlet aromatic character of SiPC ring. It is evident that the smaller ∠SiPC angles introduce enormous strain in triplet states, to the extent where the cyclic structures of $\mathbf{1}_{t\text{-}Cl}$ and $\mathbf{1}_{t\text{-}Br}$ tear down upon optimization (see Fig. 2). The trend of changes in ∠SiCP angle as a function of X in singlet $\mathbf{1}_{s\text{-}X}$ follows the size: Br > Cl > F > H (see Fig. 2). Again, this speaks for lower importance of canonical forms having C=X in $\mathbf{1}_{s\text{-}X}$ (see Scheme 1).

3.1.2. Silylenes with acyclic structures (2)

Acyclic [(X-phosphino)methylene]silylene (**2**) is more sensitive to halogens than **1**, due to its higher linearity which enhances the direct resonance effect of halogens (see Figs. 1 and 2). Higher significance of the resonance in the singlet states makes $\mathbf{2}_{s\text{-}x}$ species appear more stable than their corresponding triplet states $\mathbf{2}_{t\text{-}x}$, where X = H, F, Cl and Br (see Tables 1–4). This is in contrast to the analogues [(X-imino)methylene]silylene where the triplet state [(imino)methylene]silylene (for X = H) appears more stable than its corresponding singlet state [29]. Therefore,

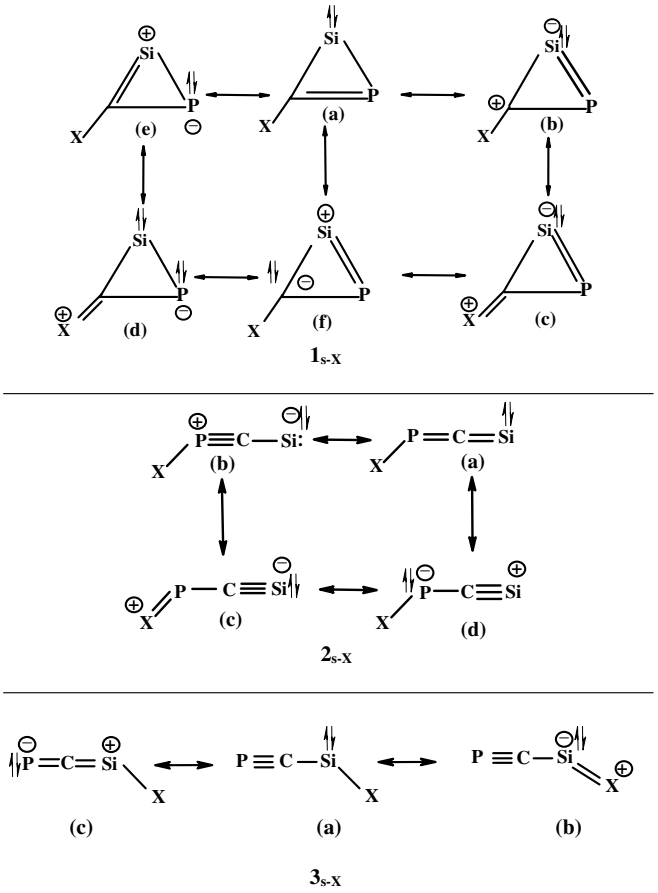

Scheme 1. Resonance canonical forms for singlet X-CPSi silylenes: $\mathbf{1}_{s\text{-}X}$, $\mathbf{2}_{s\text{-}X}$ and $\mathbf{3}_{s\text{-}X}$ (where X = H, F, Cl and Br).

going from the halo-azasilylenes X-CNSi [29] to the analogues more electropositively substituted halo-phosphasilylenes X-CPSi has reduced the chances of encountering triplet ground state silylenes. The tendency of C–N to have a higher bond order overwhelms that of C–P due to the hardness-softness properties involved. Nevertheless, the higher C–N and/or C–P bond order, the more stable are the corresponding structures H–N=C=Si: and/or H–P=C=Si:. Calculations on H–N=C=Si: show a bond order of 1.94 for the C=N in its triplet state and 1.89 in its singlet state. Hence, the triplet state of H–N=C=Si: appears about 5 kcal/mol (at B3LYP/6-311++G** [29]) more stable than its singlet state. In contrast, all calculations on H–P=C=Si: show a bond order of 1.65 for the C=P in its singlet state ($\mathbf{2}_{s\text{-}H}$) and 1.58 in its triplet state ($\mathbf{2}_{t\text{-}H}$). Hence, the singlet state of $\mathbf{2}_{s\text{-}H}$ appears about 22 kcal/mol (at CCSD(T)/6-311++G**) more stable than $\mathbf{2}_{t\text{-}H}$ (see Tables 1 and 5).

β-Halogens in **2** have less effects on their Si–C than C–P bond length (see Fig. 2). In $\mathbf{2}_{s\text{-}H}$, C–P bond length is longer than those in the halogenated $\mathbf{2}_{s\text{-}X}$ with X = F, Cl or Br. Not much of difference between C–P bond lengths in the halogenated $\mathbf{2}_{s\text{-}X}$ is observed. The ∠XPC angle, for all $\mathbf{2}_{s\text{-}X}$ isomers is larger than those in their corresponding $\mathbf{2}_{t\text{-}X}$. Again, this can be attributed to the higher importance of resonance in the singlet state which influences the linearity of singlet more than the triplet states. The higher importance of resonance stabilization of singlet states of the halo species $\mathbf{2}_{s\text{-}X}$ compared to their corresponding triplet states $\mathbf{2}_{t\text{-}X}$ is manifested through the comparison of atomic charges on the carbon atoms involved. Halogens appear to deplete atomic charges of carbons of singlet states much more than those in triplet states (see Table 5).

The order of change in ∠XPC angle, in triplet $\mathbf{2}_{t\text{-}X}$ as a function of X follows the electro-negativity: F > Cl > Br > H. One may rationalize the above data by comparing the possible resonance canonical forms of $\mathbf{2}_{s\text{-}X}$ vs. $\mathbf{2}_{t\text{-}X}$ where X = H, F, Cl and Br (see Schemes 1 and 2). All ∠SiCP angles in $\mathbf{2}_{s\text{-}X}$ are smaller than their corresponding triplets ($\mathbf{2}_{t\text{-}X}$) since linearity of Si–C–P moiety in $\mathbf{2}_{t\text{-}X}$ is more than that of $\mathbf{2}_{s\text{-}X}$. The CCSD(T)/6-311++G** calculated order of singlet–triplet energy gaps ($\Delta E_{s\text{-}t,X}$), between $\mathbf{2}_{s\text{-}X}$ and $\mathbf{2}_{t\text{-}X}$ follows the electro-negativity: $\Delta E_{s\text{-}t,F}$ (38.15 kcal/mol) > $\Delta E_{s\text{-}t,Cl}$ (33.23 kcal/mol) > $\Delta E_{s\text{-}t,Br}$ (26.83 kcal/mol]) > $\Delta E_{s\text{-}t,H}$ (22.05 kcal/mol) (see Tables 1–4). Apparently halogen stabilization of the singlet states is more pronounced in **2** than **1**.

3.1.3. Silylenes with acyclic structures (3)

Acyclic X-methylidynphosphinesilylene (**3**) is more affected by halogen substitutions than **1**, due to the direct

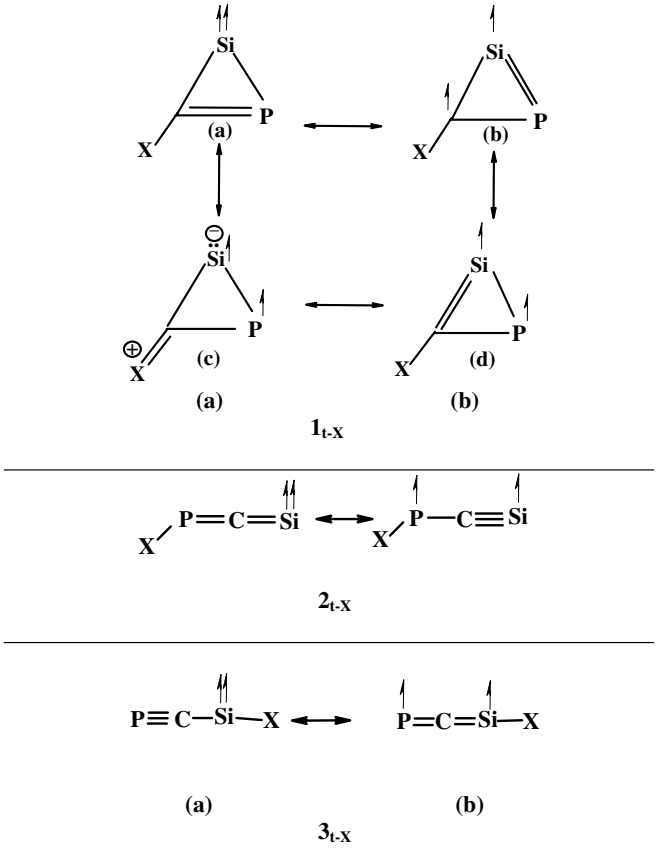

Scheme 2. Resonance canonical forms for triplet X-CPSi phosphasilylenes: $\mathbf{1}_{t\text{-}X}$, $\mathbf{2}_{t\text{-}X}$ and $\mathbf{3}_{t\text{-}X}$ (where X = H, F, Cl and Br).

attachment of the halogens to its silylenic center (see Fig. 1). Singlet $\mathbf{3}_{\mathbf{s\text{-}X}}$ (X = H, F, Cl and Br) are more stable than their corresponding triplet $\mathbf{3}_{\mathbf{t\text{-}X}}$. Among all halogenated X-CPSi species scrutinized, the lowest energy minimum appears to be the singlet $\mathbf{3}_{\mathbf{s\text{-}x}}$, while for H-CPSi isomers the lowest energy minimum is $\mathbf{1}_{\mathbf{s\text{-}H}}$. These results are in contrast to C_3HX, C_2HSiX and CNXSi previously studied by us [28,29,52]. Resonance stabilizing effect of methylidynephosphine group (C≡P) along with inductive and/or resonance effect of halogens, in both singlet and triplet states of structure **3**, can justify this trend of stability. In H-CPSi isomers (where X = H) the aromaticity in cyclic $\mathbf{1}_{\mathbf{s\text{-}H}}$ causes higher stability than conjugation of Si with CP group encountered in **2** and/or **3**. This is in contrast to the case of cyano group (C≡N), in CHNSi where conjugation of Si with CN, causes higher stability than the aromaticity in the cyclic form [29]. Singlet–triplet energy gaps between $\mathbf{3}_{\mathbf{s\text{-}X}}$ and $\mathbf{3}_{\mathbf{t\text{-}X}}$ ($\Delta E_{\mathbf{s\text{-}t,X}}$), calculated at the CCSD(T)/6-311++G** level is: $\Delta E_{\mathbf{s\text{-}t,F}}$ (44.55 kcal/mol) > $\Delta E_{\mathbf{s\text{-}t,Cl}}$ (38.60 kcal/mol) > $\Delta E_{\mathbf{s\text{-}t,Br}}$ (37.37 kcal/mol) > $\Delta E_{\mathbf{s\text{-}t,H}}$ (23.90 kcal/mol) (see Tables 1–4). This finding clearly demonstrates the stabilizing of silylenes, due to the effects of electro-negativity, suggested by Grev [22]. However, since the difference between $\Delta E_{\mathbf{s\text{-}t,Cl}}$ and $\Delta E_{\mathbf{s\text{-}t,Br}}$ is small one can conclude that resonance effects of halogens also act as an stabilizing effect on the divalent center. Generally, $\Delta E_{\mathbf{s\text{-}t}}$ in structure **3** is more than that in structure **2**. MP2 and B3LYP calculations suggest Si–C bond length to be longer for singlet isomers than their corresponding triplet states (see Fig. 2).The ∠CSiX angle in **3** increases as a function of the size of X: Br > Cl > F > H (see Fig. 2). On the other hand, as expected ∠CSiX angle for all singlet states is smaller than their corresponding triplets. Linearity of P–C–Si moiety in triplets is higher than their corresponding singlet states. One of the significant parameters affecting the $\Delta E_{\mathbf{s\text{-}t}}$ and determining the ground state of silylenes and/or carbenes is the magnitude of divalent bond angle. Therefore, bending potential energy curves for divalent $\mathbf{3}_{\mathbf{s\text{-}X}}$ and $\mathbf{3}_{\mathbf{t\text{-}X}}$ species are calculated at B3LYP/6-311++G** (see Fig. 5). All the substituents X employed increase the angle which singlet and triplet states cross. The order of the singlet–triplet cross-points as a function of X follows electro-negativity: F (no clear cross-point) > Cl ≈ Br(150°) > H (140°). One may wonder how the cross over diagrams can help in designing triplet silylenes. Evidently, employing trialkylsilyl groups as substituents, simultaneously electropositive and bulky, may enable the angle at the divalent silicon atom to surpass where the triplet becomes lower in energy than the singlet.

To gain more insight into the relative stability trends obtained for silylenes **1**–**3**, three different isodesmic reactions are considered which are depicted on the bottom of Table 6. Isodesmic reactions for cyclic structures **1** show some stabilization of these species due to aromaticity, while those of acyclic structures **2** and **3** show higher stabilizations through resonance. Isodesmic reactions suggest that $\mathbf{1}_{\mathbf{s\text{-}H}}$ is somewhat more stable than $\mathbf{1}_{\mathbf{t\text{-}H}}$ (see Table 6). Both F and Cl increase the stability of the singlets $\mathbf{1}_{\mathbf{s\text{-}F}}$ and $\mathbf{1}_{\mathbf{s\text{-}Cl}}$ more than their corresponding triplets ($\mathbf{1}_{\mathbf{t\text{-}F}}$ and $\mathbf{1}_{\mathbf{t\text{-}Cl}}$), while Br somewhat destabilize the singlet $\mathbf{1}_{\mathbf{s\text{-}Br}}$. For acyclic structures **3**, triplet states $\mathbf{3}_{\mathbf{t\text{-}X}}$ are more stable than their

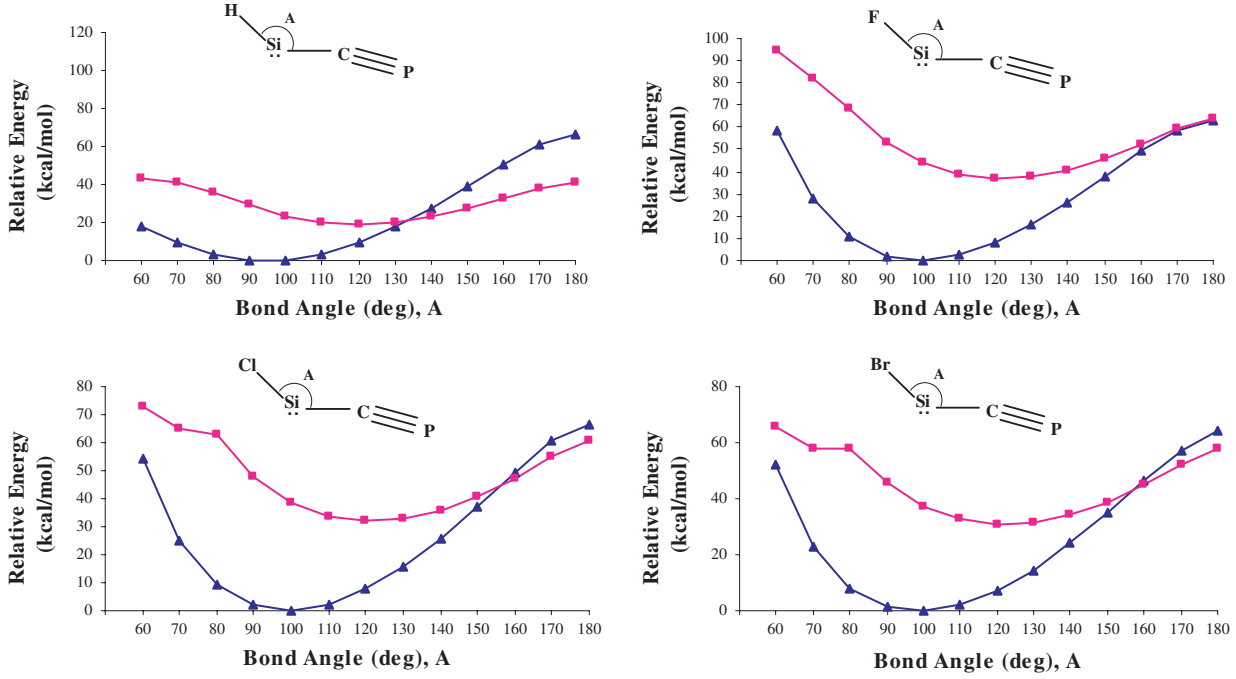

Fig. 5. Crossing of the singlet ($\mathbf{3}_{\mathbf{s\text{-}X}}$, ▲) and triplet ($\mathbf{3}_{\mathbf{t\text{-}X}}$, ■) states through plotting their B3LYP/6-311++G** relative energies (kcal/mol) against their corresponding divalent bond angle ∠XSiC or *A* (°) (where X = H, F, Cl and Br).

Table 6
B3LYP/6-311++G** calculated enthalpies (kcal/mol), for isodesmic reactions of singlet (**s**) and triplet (**t**) X-CPSi silylenes, **1**–**3**

Structure	ΔH[a]	Structure	ΔH[b]	Structure	ΔH[c]
$\mathbf{1}_{s\text{-}H}$	15.10	$\mathbf{2}_{s\text{-}H}$	8.20	$\mathbf{3}_{s\text{-}H}$	17.11
$\mathbf{1}_{t\text{-}H}$	13.37	$\mathbf{2}_{t\text{-}H}$	93.44	$\mathbf{3}_{t\text{-}H}$	20.67
$\mathbf{1}_{s\text{-}F}$	14.92	$\mathbf{2}_{s\text{-}F}$	72.60	$\mathbf{3}_{s\text{-}F}$	11.63
$\mathbf{1}_{t\text{-}F}$	−0.48	$\mathbf{2}_{t\text{-}F}$	6.24	$\mathbf{3}_{t\text{-}F}$	19.28
$\mathbf{1}_{s\text{-}Cl}$	13.85	$\mathbf{2}_{s\text{-}Cl}$	50.05	$\mathbf{3}_{s\text{-}Cl}$	12.94
$\mathbf{1}_{t\text{-}Cl}$	4.31	$\mathbf{2}_{t\text{-}Cl}$	44.81	$\mathbf{3}_{t\text{-}Cl}$	19.07
$\mathbf{1}_{s\text{-}Br}$	12.35	$\mathbf{2}_{s\text{-}Br}$	72.03	$\mathbf{3}_{s\text{-}Br}$	13.36
$\mathbf{1}_{t\text{-}Br}$	17.10	$\mathbf{2}_{t\text{-}Br}$	67.25	$\mathbf{3}_{t\text{-}Br}$	19.17

[a] Based on the following isodemic reaction:

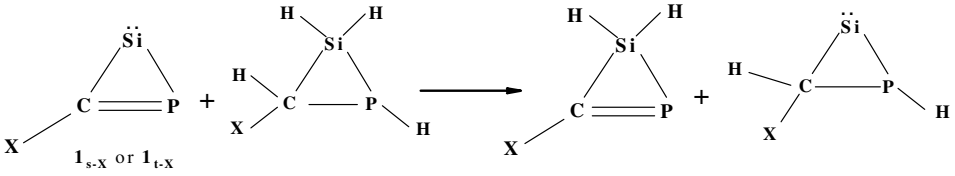

[b] Based on:

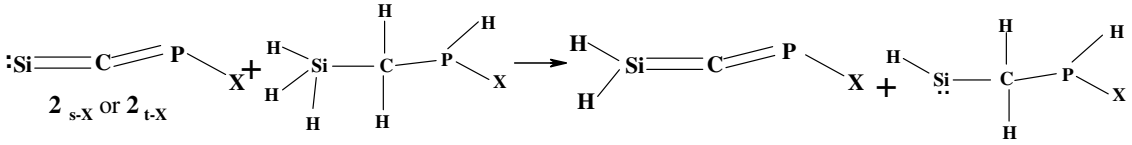

[c] Based on:

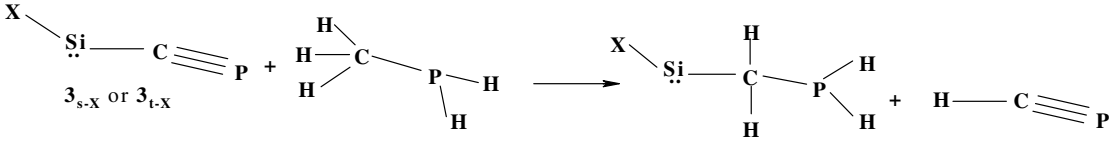

corresponding singlet states ($\mathbf{3}_{s\text{-}X}$), due to resonance stabilization effects of C≡P triple bonds. The higher the electronegativity of X, the greater is the energy difference between $\mathbf{3}_{t\text{-}X}$ and $\mathbf{3}_{s\text{-}X}$ species. While triplet $\mathbf{2}_{t\text{-}H}$ is considerably more stable than singlet $\mathbf{2}_{s\text{-}H}$, other triplet states $\mathbf{2}_{t\text{-}X}$ are less stable than their corresponding singlet states $\mathbf{2}_{s\text{-}X}$ where X = F, Cl and Br (see Table 6). Isodesmic reactions for cyclic structures of halo-azasilylenes (X-SiNC), $\mathbf{1}_{s\text{-}X}$ and $\mathbf{1}_{t\text{-}X}$, show triplet $\mathbf{1}_{t\text{-}H}$ more stable than singlet $\mathbf{1}_{s\text{-}H}$, while other triplet states $\mathbf{1}_{t\text{-}X}$ are less stable than their corresponding singlet states $\mathbf{1}_{s\text{-}X}$, where X = F, Cl and Br (see Table 7). In order to improve measurement of aromaticity and/or anti-aromaticity of the species scrutinized, nucleus independent chemical shift NICS values [54] are also calculated for cyclic species of X-SiCP and X-SiCN (see Tables 8 and 9). NICS (1) (i.e., at points 1 Å above the ring center) was

Table 7
B3LYP/6-311++G** calculated enthalpies (kcal/mol), for isodesmic reactions of cyclic singlet (**s**) and triplet (**t**) X-CNSi silylenes **1**

Structure	$\mathbf{1}_{s\text{-}H}$	$\mathbf{1}_{t\text{-}H}$	$\mathbf{1}_{s\text{-}F}$	$\mathbf{1}_{t\text{-}F}$	$\mathbf{1}_{s\text{-}Cl}$	$\mathbf{1}_{t\text{-}Cl}$	$\mathbf{1}_{s\text{-}Br}$	$\mathbf{1}_{t\text{-}Br}$
ΔH^a	−0.14	1.28	−1.76	−10.55	−2.61	−4.76	−1.42	−0.92

Table 8
NICS (total) values (ppm) of singlet (s) states of cyclic halo-aza silylenes X-SiCN ($1_{s\text{-}X}$ and $1_{t\text{-}X}$) (X = H, F, Cl and Br) [29], calculated at ring centers as well as 0.5, 1, 1.5, 2, 2.5 and 3 Å above; at GIAO-B3LYP/6-311++G**//B3LYP/6-311++G** level

Structure	NICS(0.5)	NICS(1)	NICS(1.5)	NICS(2)	NICS(2.5)	NICS(3)
$\mathbf{1}_{s\text{-}H}$	−18.8	−14.0	−7.4	−4.0	−2.4	−1.6
$\mathbf{1}_{s\text{-}F}$	−22.3	−13.0	−5.8	−2.8	−1.5	−1.0
$\mathbf{1}_{s\text{-}Cl}$	−20.0	−12.8	−6.1	−3.1	−1.8	−1.2
$\mathbf{1}_{s\text{-}Br}$	−19.2	−12.3	−5.9	−3.0	−1.8	−1.2

Table 9
NICS (total) values (ppm) of singlet (s) states of cyclic halo-phospha silylenes X-SiCP ($\mathbf{1_{s\text{-}X}}$) (X = H, F, Cl and Br), calculated at ring centers as well as 0.5, 1, 1.5, 2, 2.5 and 3 Å above; at GIAO-B3LYP/6-311++G**//B3LYP/6-311++G** level

Structure	NICS(0)	NICS(0.5)	NICS(1)	NICS(1.5)	NICS(2)	NICS(2.5)	NICS(3)
$\mathbf{1_{s\text{-}H}}$	−10.3	−16.6	−15.0	−9.1	−5.2	−3.2	−2.1
$\mathbf{1_{s\text{-}F}}$	−13.8	−18.2	−14.2	−7.6	−3.9	−2.3	−1.4
$\mathbf{1_{s\text{-}Cl}}$	−12.1	−17.4	−14.4	−8.1	−4.4	−2.6	−1.7
$\mathbf{1_{s\text{-}Br}}$	−11.4	−16.9	−14.1	−7.9	−4.3	−2.6	−1.7

recommended as being a better measure of the π electron delocalization as compared to NICS(0) (i.e., at the ring center) [55]. Interestingly, the NICS values indicate that all singlet cyclic silylenes show aromatic character for having negative NICS values (see Tables 7 and 8). Halogens rather decrease the aromaticity of $\mathbf{1_{s\text{-}X}}$. The aromatic character of cyclic singlet azasilylenes are lower than their analogues phosphasilylenes, as predicted by isodesmic reactions (see Tables 6–9). Moreover, the aromatic character of $\mathbf{1_{s\text{-}X}}$ species are higher than that of benzene ring (NICS(1) = −10.6 ppm) [55,56]. While using isodesmic reactions can validate theoretical methods, but different isodesmic reactions give different results without one being systematically better than the other [57]. Comparison of data from isodesmic reactions with those of NICS reveal that the latter values are more reliable for assessing the aromatic stability of cyclic systems employed in this study.

3.2. NBO analysis

The NBO method represents the electronic structure of a molecule in terms of the best possible resonance Lewis structure. The NBO analysis shows that in all cyclic structures divalent Si atom has positive charges. Positive charges on Si atom in all the triplet $\mathbf{1_{t\text{-}X}}$ species are larger than their corresponding singlet states $\mathbf{1_{s\text{-}X}}$.

The changes of charges on the divalent center as a function of substituents, can clearly presented with drawing plots of atomic charges on Si atom vs. Swain and Lupton constants [58] including polar (F) and/or resonance (R) constants for three silylenic structures **1**–**3** (see Fig. 6). A significant point concerns the atomic charges on the divalent Si atom of $\mathbf{1_{s\text{-}X}}$, $\mathbf{1_{t\text{-}X}}$, $\mathbf{3_{s\text{-}X}}$ and $\mathbf{3_{t\text{-}X}}$ which appear to have better linear relationships with the R constants than their corresponding F constants. In contrast, $\mathbf{2_{s\text{-}X}}$ and $\mathbf{2_{t\text{-}X}}$ appear to have better linear relationships with the F than the R constants (see Fig. 6). Moreover, the linear relationships of singlet state $\mathbf{2_{s\text{-}X}}$ vs. F ($R^2 = 0.99$), and the linear relationships of singlet state $\mathbf{3_{s\text{-}X}}$ vs. R ($R^2 = 0.98$) are remarkable. This results indicates that for acyclic structures **2**, inductive effects of substituents attached the divalent center are more important than their corresponding resonance effects.

3.3. Effects of the nature of the divalent center on singlet–triplet energy gaps, $\Delta E_{s\text{-}t}$

Equally important is the effect of the nature of the divalent center (carbene vs. silylene vs. germylene) on the magnitude of the corresponding singlet–triplet energy gaps, $\Delta E_{s\text{-}t}$. Comparison is made between the B3LYP/6-311++G** calculated singlet–triplet energy separations, $\Delta E_{s\text{-}t}$ (kcal/mol) of X-substituted C_2PX carbenes [59], SiCPX silylenes and GeCPX germylenes [60] which are confined to three structures: (a) cyclic structures 3-X-2-phospha-1-M-cyclopropenylidene ($\mathbf{1_{s\text{-}X}}$ vs. $\mathbf{1_{t\text{-}X}}$); (b) acyclic structure [(X-phosphino)methylene]-M-ylidene $\mathbf{2_{s\text{-}X}}$ vs. $\mathbf{2_{t\text{-}X}}$; (c) acyclic structure X-methylidynephosphine-M-ylidene ($\mathbf{3_{s\text{-}X}}$ vs. $\mathbf{3_{t\text{-}X}}$), for M = C, Si and Ge, where X = H, F, Cl and Br (see Fig. 7). While the relative sensitivity of $\Delta E_{s\text{-}t}$ for acyclic structures **2**, are less affected by different divalent centers (see Fig. 7a), it is more pronounced for structure **1** (see Fig. 7b), and is the most conspicuous for acyclic structures **3** (see Fig. 7c). Such a high resolution

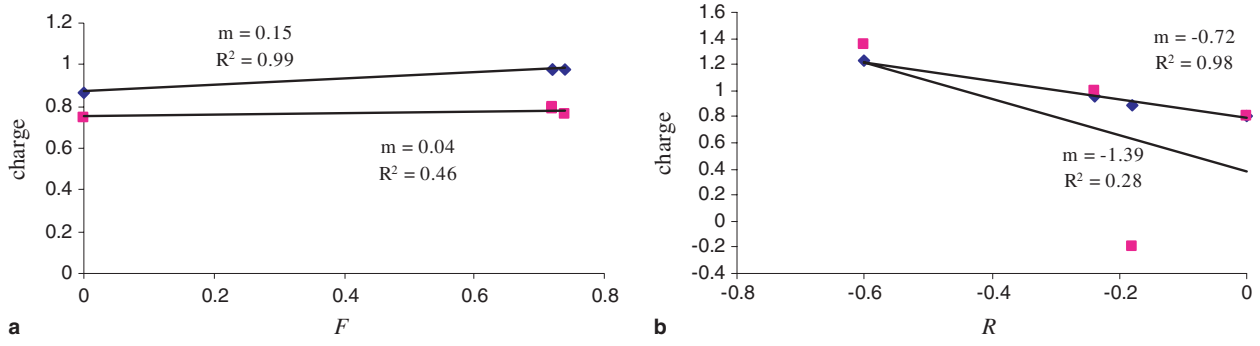

Fig. 6. Plots of NBO atomic charges on silylenic center vs. polar (F) and resonance (R) (Swain and Lupton constants [58]), for singlet (▲) and triplet (■) states of silylenic X-CPSi ($\mathbf{2_{s\text{-}X}}$ vs. $\mathbf{2_{t\text{-}X}}$ diagram a) and ($\mathbf{3_{s\text{-}X}}$ vs. $\mathbf{3_{t\text{-}X}}$ diagram b), X = H, F, Cl and Br (see Table 5) (R^2 = correlation coefficient, m = curve slope).

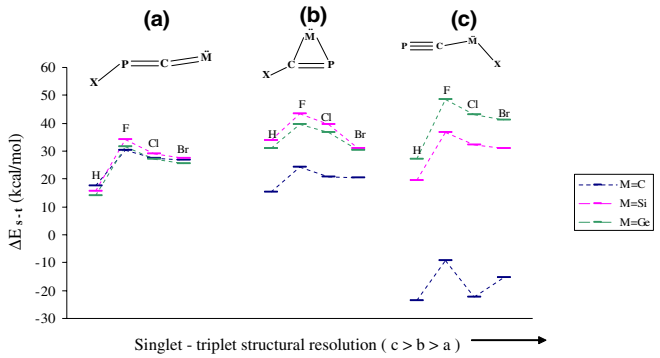

Fig. 7. Comparison of B3LYP/6-311++G** calculated singlet–triplet energy gaps $\Delta E_{s\text{-}t}$ (kcal/mol) between X-substituted C_2PX carbenes (−) [59], SiCPX silylenes (−) and GeCPX germylenes (−) [60] confined to three structures: (a) acyclic structure [(X-phosphino)methylene]-M-ylidene $\mathbf{2}_{s\text{-}X}$ vs. $\mathbf{2}_{t\text{-}X}$; (b) cyclic structures 3-X-2-phospha-1-M-cyclopropenylidene ($\mathbf{1}_{s\text{-}X}$ vs. $\mathbf{1}_{t\text{-}X}$); (c) acyclic structures X-methylidynephosphine-M-ylidene ($\mathbf{3}_{s\text{-}X}$ vs. $\mathbf{3}_{t\text{-}X}$), for M = C, Si and Ge, where X = H, F, Cl and Br.

observed in Fig. 7c is possibly due to the different distances between divalent centers and the stabilizing C≡P groups, regardless of the substituent X employed. The highest calculated $\Delta E_{s\text{-}t}$ for cyclic aromatic structures **1** appears to be those of silylenes SiCPX. On the other hand, the highest $\Delta E_{s\text{-}t}$ for acyclic structures **3** is for the most electropositive germylenes GeCPX.

4. Conclusion

Singlet–triplet energy separation ($\Delta E_{s\text{-}t,X}$) in the silylenic reactive intermediates X-CPSi, are compared and contrasted, at eight high levels of ab initio and DFT methods (where X = H, F, Cl and Br). Three possible structures anticipated for each singlet (**s**) and/or triplet (**t**) silylene, X-CPSi, are: 3-X-2-phospha-1-silacyclopropenylidene (**1**), [(X-phosphino)methylene]silylene (**2**), and X-methylidynphosphinesilylene (**3**). All silylenic species studied are real isomers with no negative force constant. The order of singlet–triplet energy separations for all cyclic and acyclic species, $\mathbf{1}_{t\text{-}X}$–$\mathbf{1}_{s\text{-}X}$, $\mathbf{2}_{t\text{-}X}$–$\mathbf{2}_{s\text{-}X}$ and $\mathbf{3}_{t\text{-}X}$–$\mathbf{3}_{s\text{-}X}$, as a function of X, follows electro-negativity: F > Cl > Br > H. Even though all singlet isomers seem to be more stable than their corresponding triplets, singlet–triplet cross over diagrams for $\mathbf{3}_{s\text{-}X}$ and $\mathbf{3}_{t\text{-}X}$, help design of new triplet state silylenes. For the six species with X = H (H-CPSi), stability order is: $\mathbf{1}_{s\text{-}H} > \mathbf{3}_{s\text{-}H} > \mathbf{2}_{s\text{-}H} > \mathbf{1}_{t\text{-}H} > \mathbf{3}_{t\text{-}H} > \mathbf{2}_{t\text{-}H}$. Likewise, stability order for the twelve isomers with X = F and Br, is: $\mathbf{3}_{s\text{-}X} > \mathbf{1}_{s\text{-}X} > \mathbf{2}_{s\text{-}X} > \mathbf{3}_{t\text{-}X} > \mathbf{2}_{t\text{-}X} > \mathbf{1}_{t\text{-}X}$. Finally, the order of stability for six isomers of Cl-CPSi is: $\mathbf{3}_{s\text{-}Cl} > \mathbf{1}_{s\text{-}Cl} > \mathbf{2}_{s\text{-}Cl} > \mathbf{3}_{t\text{-}Cl} > \mathbf{1}_{t\text{-}Cl} > \mathbf{2}_{t\text{-}Cl}$. Linear correlations are found between the LUMO–HOMO energy gaps of the singlet X-CPSi silylenes, and their corresponding singlet–triplet energy separations calculated at B3LYP/6-311++G**. The lowest energy minimum, among six H-CPSi species scrutinized, appears to be the singlet cyclic $\mathbf{1}_{s\text{-}H}$. However the lowest energy minima, among all X-CPSi (X = F, Cl and Br) species, appears to be the singlet acyclic $\mathbf{3}_{s\text{-}X}$. Among all halo-silylenes studied, the acyclic structure **2** appears to be the most polar species.

Acknowledgements

We are grateful to A. Ghaderi (Imam Hossein University); Mahnaz and Mehran Ghambarian (Sharif University of Technology); Dr. Y. Fatholahi, S. Souri, S.E. Hosseini, H. Hamadi and H.R. Mahzooni (Chemistry Department, Tarbiat Modares University) for many stimulating and helpful discussions as well as technical assistance.

Appendix A. Supplementary data

Supplementary data associated with this article can be found, in the online version, at doi:10.1016/j.jorganchem.2006.01.059.

References

[1] P.P. Gaspar, R. West, in: Z. Rappoport, Y. Apeloig (Eds.), The Chemistry of Organic Silicon Compounds, second ed., Wiley, Chichester, 1998, p. 2463 (Part 3, Chapter 43).
[2] J. Barrau, J. Escudie, J. Satge, Chem. Rev. 90 (1990) 283.
[3] M.F. Lappert, Coord. Chem. Rev. 100 (1990) 267.
[4] W.P. Neumann, Chem. Rev. 91 (1991) 311.
[5] M.F. Lappert, Main Group Met. Chem. 17 (1994) 183.
[6] J. Barrau, G. Rima, Coord. Chem. Rev. 178 (1998) 593.
[7] M. Haaf, T.A. Schmedake, R. West, Acc. Chem. Res. 33 (2000) 704.
[8] N. Tokitoh, R. Okazaki, Coord. Chem. Rev. 210 (2000) 251.
[9] B. Gehrhus, M.F. Lappert, J. Organomet. Chem. 61 (2001) 209.
[10] T.J. Drahnak, J. Michl, R. West, J. Am. Chem. Soc. 101 (1979) 5427.
[11] M. Denk, R. Lennon, R. Hayashi, R. West, A. Haaland, H. Belyakov, P. Verne, M. Wagner, N. Metzler, J. Am. Chem. Soc. 116 (1994) 2691.
[12] N. Takeda, H. Suzuki, N. Tokitoh, R. Okazaki, S. Nagase, J. Am. Chem. Soc. 119 (1997) 1456.
[13] M. Kira, S. Ishida, T. Iwamoto, C. Kabuto, J. Am. Chem. Soc. 121 (1999) 9722.
[14] P.P. Gaspar, M. Xiao, D. Ho Pae, D.J. Berger, T. Haile, T. Chen, D. Lei, W.R. Winchester, P. Jiang, J. Organomet. Chem. 646 (2002) 68.
[15] B.T. Luke, J.A. Pople, M.B. Krogh-Jespersen, Y. Apeloig, M. Karni, J. Chandrasekhar, P.v.R. Schleyer, J. Am. Chem. Soc. 108 (1986) 270.
[16] M.S. Gordon, D. Bartol, J. Am. Chem. Soc. 109 (1987) 5948.
[17] J.L. Berkowitz, J.P. Green, H. Cho, R. Ruscic, J. Chem. Phys. 86 (1987) 1235.
[18] R. Grev, H.F. Schaefer III, J. Chem. Phys. 97 (1992) 8389.
[19] D.R. Rao, J. Mol. Spectrosc. 34 (1970) 284.
[20] R.S. Grev, H.F. Schaefer III, J. Am. Chem. Soc. 108 (1986) 5804.
[21] K. Krogh-Jespersen, J. Am. Chem. Soc. 107 (1985) 537.
[22] R.S. Grev, H.F. Schaefer III, P.P. Gaspar, J. Am. Chem. Soc. 113 (1991) 5638.
[23] M.E. Colvin, H.F. Schaefer III, J. Bicerano, J. Chem. Phys. 83 (1985) 4581.
[24] M.E. Colvin, J. Breulet, H.F. Schaefer III, Tetrahedron 41 (1985) 1429.
[25] M.C. Holthausen, W. Koch, Y. Apeloig, J. Am. Chem. Soc. 121 (1999) 2623.
[26] A. Sekiguchi, T. Tanaka, M. Ichinohe, K. Akiyama, S. Tero-Kubota, J. Am. Chem. Soc. 125 (2003) 4962.
[27] M.Z. Kassaee, S.M. Musavi, M. Ghambarian, J. Organomet. Chem. (accepted for publication).
[28] M.Z. Kassaee, S.M. Musavi, F. Buazar, M. Ghambarian, J. Mol. Struct. (Theochem) 722 (2005) 151.

[29] M.Z. Kassaee, S.M. Musavi, H. Hamadi, M. Ghambarian, S.E. Hosseini, J. Mol. Struct. (Theochem) 730 (2005) 33.
[30] A.J. Apponi, M.C. McCarthy, C.A. Gottlieb, P. Thaddeus, Astrophys. J. (2000) 536.
[31] J. Furthmller, F. Bechstedt, H. Hsken, B. Schrter, W. Richter, Phys. Rev. B 58 (L1) (1998) 13712.
[32] M. Weidenbruch, Chem. Rev. 95 (1995) 1479.
[33] Y. Apeloig, M. Karni, Organometallics 16 (1997) 310.
[34] Y. Apeloig, M. Karni, Theoretical aspects and quantum chemical calculation of silaaromatic compounds, in: Z. Pappoport, Y. Apeloig (Eds.), The Chemistry of Silicon Compounds, vol. 2, Wiley, New York, 1998, pp. 1–120.
[35] A. Sekiguchi, R. Kinjo, M. Ichinohe, Science 305 (2004) 1755.
[36] T. Iwamoto, D. Yin, C. Kabuto, M. Kira, J. Am. Chem. Soc. 123 (2001) 12730.
[37] Y. Kon, J. Ogasawara, K. Sakamoto, C. Kabuto, M. Kira, J. Am. Chem. Soc. 125 (2003) 9310.
[38] S. Ishida, T. Iwamoto, D. Yin, C. Kabuto, M. Kira, Nature 421 (2003) 725.
[39] M.Z. Kassaee, M. Ghambarian, S.M. Musavi, J. Organomet. Chem. 690 (2005) 3427.
[40] M.J. Frisch, G.W. Trucks, H.B. Schlegel, G.E. Scuseria, M.A. Robb, J.R. Cheeseman, V.G. Zakrzewski Jr., J.A. Montgomery, R.E. Stratmann, J.C. Burant, S. Dapprich, J.M. Millan, A.D. Daniels, K.N. Kudin, M.C. Strain, O. Farkas, J. Tomasi, V. Barone, M. Cossi, R. Cammi, B. Mennucci, C. Pomelly, C. Adamo, S. Clifford, J. Ochterski, G.A. Petersson, P.Y. Ayala, Q. Cui, K. Morokuma, D.K. Malick, A.D. Rabuck, K. Raghavachari, J.B. Foresman, J. Cioslowski, J.V. Ortiz, A.G. Baboul, B.B. Stefanov, G. Liu, A. Liashenko, P. Piskorz, I. Komaromi, R. Gomperts, R.L. Martin, D.J. Fox, T. Keith, M.A. Al-Laham, C.Y. Peng, A. Nanayakkara, C. Gonzalez, M. Challacombe, P.M.W. Gill, B. Johnson, W. Chen, M.W. Wong, J.L. Andres, C. Gonzalez, M. Head-Gordon, E.S. Replogle, J.A. Pople, GAUSSIAN 98, Revision A.6, Gaussian, Inc., Pittsburgh, PA, 1998.
[41] A.D. Becke, J. Chem. Phys. 104 (1996) 1040.
[42] C. Adamo, V. Barone, Chem. Phys. Lett. 274 (1997) 242.
[43] S. Saebo, J. Almlof, Chem. Phys. Lett. 154 (1989) 83.
[44] J.A. Pople, J.S. Binkley, R. Seeger, Int. J. Quant. Chem. Symp. 10 (1976) 1.
[45] J.A. Pople, R. Krishnan, Int. J. Quant. Chem. 14 (1978) 91.
[46] R. Krishnan, M.J. Frisch, J.A. Pople, J. Chem. Phys. 72 (1980) 4244.
[47] J.A. Pople, M. Head-Gordon, K. Raghavachari, J. Chem. Phys. 87 (1987) 5968.
[48] G.E. Scuseria, H.F. Schaefer III, J. Chem. Phys. 90 (1989) 3700.
[49] R.F. Hout, B.A. Levi, W.J. Heher, J. Comput. Chem. 82 (1985) 234.
[50] D.J. Defrees, A.D. McLean, J. Chem. Phys. 82 (1985) 333.
[51] J.E. Carpenter, F. Weinhold, J. Mol. Struct. (Theochem) 41 (1988) 169.
[52] M.Z. Kassaee, B.N. Haerizade, S. Arshadi, J. Mol. Struct. (Theochem) 639 (2003) 187.
[53] Y. Apeloig, R. Pauncz, M. Karni, R. West, W. Steiner, D. Chapman, Organometallics 22 (2003) 3250.
[54] P.v.R. Schleyer, C. Maerker, A. Dransfeld, H. Jiao, N.J.R.v.E. Hommes, J. Am. Chem. Soc. 118 (1996) 6317.
[55] P.v.R. Schleyer, M. Manoharan, Z.X. Wang, B. Kiran, H. Jiao, R. Puchta, N.J.R.v.E. Hommes, Org. Lett. 3 (2001) 2465.
[56] M.N. Glukhovtsev, L. Sergei, P. Addy, J. Phys. Chem. 100 (1996) 17801.
[57] W.J. Hehre, R. Ditchfield, L. Radom, J.A. Pople, J. Am. Chem. Soc. 92 (1970) 4796.
[58] C.G. Swain, C.E. Lupton Jr., J. Am. Chem. Soc. 90 (1968) 4328.
[59] M.Z. Kassaee, S.M. Musavi, M. Ghambarian, F. Buazar, J. Mol. Struct. (Theochem) 726 (2005) 171.
[60] M.Z. Kassaee, S.M. Musavi, M. Ghambarian, J. Mol. Struct. (Theochem) (submitted for publication).